Med Chem Res (2013) 22:1825–1836
DOI 10.1007/s00044-012-0180-1

MEDICINAL CHEMISTRY RESEARCH

ORIGINAL RESEARCH

Tetracyclic spirooxindole blockers of $hNa_V1.7$: activity in vitro and in CFA-induced inflammatory pain model

Sultan Chowdhury · Shifeng Liu · Jay A. Cadieux · Tom Hsieh · Mikhail Chafeev · Shaoyi Sun · Qi Jia · Jianyu Sun · Mark Wood · Jonathan Langille · Serguei Sviridov · Jianmin Fu · Zaihui Zhang · Ray Chui · Audrey Wang · Xing Cheng · Jing Zhong · Sazzad Hossain · Kuldip Khakh · Ivana Rajlic · Henry Verschoof · Rainbow Kwan · Wendy Young

Received: 6 January 2012 / Accepted: 21 July 2012 / Published online: 12 August 2012

Abstract The structure–activity relationship of a new series of tetracyclic spirooxindoles led to the discovery of compound **25a**, a potent $hNa_V1.7$ blocker with improved ADME properties and in vivo efficacy in the CFA-induced inflammatory pain model.

Keywords Sodium channel blockers · $Na_V1.7$ blockers · Pain · Tetracyclic spirooxindole · Methylenedioxy · Mitsunobu reaction

Abbreviations

$hNa_V1.7$	human sodium channel 1.7 subtype
CYP	Cytochrome P450
DMF	*N*,*N*-Dimethylformamide
CFA	Complete Freund's adjuvant
IP	Intraperitoneal
TMSCl	Chlorotrimethylsilane
THF	Tetrahydrofuran
MOMCl	Chloromethoxymethyl ether
tert-BuLi	*tert*-butyllithium
TFA	Trifluoroacetic acid
ADME	Absorption, distribution, metabolism, and excretion

S. Chowdhury (✉) · S. Liu · J. A. Cadieux · T. Hsieh · M. Chafeev · S. Sun · Q. Jia · J. Sun · M. Wood · J. Langille · S. Sviridov · J. Fu · Z. Zhang
Department of Medicinal Chemistry, Xenon Pharmaceuticals Inc., 3650 Gilmore Way, Burnaby, BCV5G 4W8, Canada
e-mail: schowdhury@xenon-pharma.com

R. Chui · A. Wang · X. Cheng · J. Zhong · S. Hossain · K. Khakh · I. Rajlic · H. Verschoof · R. Kwan · W. Young
Department of Biological Sciences, Xenon Pharmaceuticals Inc., 3650 Gilmore Way, Burnaby, BCV5G 4W8, Canada

Introduction

$hNa_V1.7$ is one of the voltage-gated sodium channel subtypes involved in pain conditions and is considered an important therapeutic target for pharmaceutical intervention based on compelling genetic evidence (Cummins *et al.*, 2007). $hNa_V1.7$ is mainly expressed in the peripheral nervous system (Klugbauer *et al.*, 1995; Toledo-Aral *et al.*, 1997; Sangameswaran *et al.*, 1997). There are many scientific reports describing the critical role of the $hNa_V1.7$ subtype in the perception of pain sensations, especially in inflammatory contexts (Goldberg *et al.*, 2007; Cox *et al.*, 2006; Reimann *et al.*, 2010; Zhang *et al.*, 2010) and may represent an important target for analgesic/anti-hyperalgesic drugs (Ghelardini *et al.*, 2010). Studies have shown that loss-of-function mutations in $hNa_V1.7$ are associated with congenital insensitivity to painful stimuli (Yang *et al.*, 2004; Cummins *et al.*, 2004; Fertleman *et al.*, 2006). Several marketed drugs used in the treatment of neuropathic pain, such as carbamazepine, oxcarbazepine, lidocaine, lamotrigine, topiramate, and mexiletine, are either weak sodium channel antagonists or possess alternate mechanisms of action which limit their clinical efficacy side effect profiles (Zuliani *et al.*, 2010). Our goal is to develop more potent, state-dependent $hNa_V1.7$ blockers for the treatment of pain.

Recently, we reported the discovery of XEN907 (**1**), a novel pentacyclic spirooxindole blocker of $hNa_V1.7$ (Chowdhury *et al.*, 2011). This compound showed high in vitro $hNa_V1.7$ potency, moderate bioavailability in male Lewis rats and poor solubility in phosphate-buffered saline (Fig. 1). XEN907 (**1**) also showed moderate hepatocyte stability across species and significant inhibition of CYP3A4 was observed in a recombinant human enzyme assay. These results prompted us to direct our medicinal

Fig. 1 Structure and ADME properties of **XEN907** (**1**)

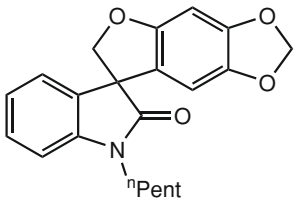

XEN907 (**1**)

IC_{50} ($hNa_V1.7$) = 3 nM
clogP = 3.97
Solubility = 7.3 μg/mL (phosphate-buffered saline @ pH 7.4)
PPB (rat) = 97%
Cytotox: > 99%
Heptocyte stability = 21% (rat)/34% (human)/46% (dog)
F =13% (*po* @10 mg/kg)

chemistry efforts to evaluate tetracyclic analogs lacking the methylenedioxy moiety which is presumably responsible for CYP induction (Staack and Maurer, 2005; Castro *et al.*, 2003; Imperio *et al.*, 2007).

Results and discussion

In order to establish a structure–activity relationship for surrogates of the methylenedioxy moiety, we designed and synthesized a series of analogs modifying the head group of the spirooxindole scaffold (Table 1). In order to decrease the electron density of the aryl head group in an effort to reduce the extent of oxidative metabolism, a number of electron-withdrawing substituents were explored. While compounds **8a** and **8b** bearing fluorine and methoxy substituents were 20- and 80-fold less potent in vitro against $hNa_V1.7$ versus compound **1**, they did demonstrate reduced CYP3A4 inhibition. A further reduction in CYP3A4 inhibition could be obtained by introducing a polar (pyridin-2-yl)methyl substituent at the *N*-position (compound **8c**). Compared to the 3,4-difluorophenyl

Table 1 Structure-activity relationship of spirooxindoles (**1**, **8a–8n**)

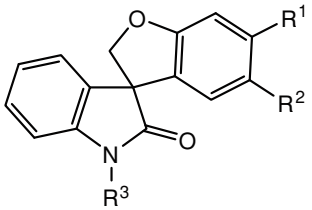

Compound	R^1	R^2	R^3	$hNa_V1.7$[a] IC_{50} (μM)	CYP3A4, % inhibition at 10 μM[b]	Solubility[c] (μg/mL)
1	$–OCH_2–$	–O–	*n*-pentyl	0.003	97	7.3
8a	F	F	*n*-pentyl	0.24	50	<5
8b	OCH_3	H	*n*-pentyl	0.06	64	<5
8c	F	F	(Pyridin-2-yl)methyl	0.27	30	13
8d	OCH_3	H	(Pyridin-2-yl)methyl	0.008	29	25
8e	OCH_3	F	(Pyridin-2-yl)methyl	0.19	36	15
8f	F	OCH_3	(Pyridin-2-yl)methyl	0.47	16	36
8g	CH_3	CH_3	(Pyridin-2-yl)methyl	0.23	43	6
8h	OCH_3	CH_3	(Pyridin-2-yl)methyl	1.15	61	7
8i	$O(CH_2)_2OCH_3$	H	(Pyridin-2-yl)methyl	0.15	22	46
8j	OCH_3	H	(Tetrahydro-2*H*-pyran-2-yl)methyl	0.01	35	14
8k	OCH_3	H	((*R*)-Tetrahydrofuran-2-yl)methyl	0.11	18	45
8l	OCH_3	F	(5-(Trifluoromethyl)furan-2-yl)methyl	0.43	69	<5
8m	OCH_3	OCH_3	(5-Chlorothiophen-2-yl)methyl	0.70	75	8
8n	F	CN	(3-(Trifluoromethyl)-pyridin-2-yl) methyl	>1.0	10	<5

[a] [^{14}C]guanidinium influx assay adapted for use in HEK-293 cells expressing human $Na_V1.7$ (Reddy *et al.*, 1998)

[b] Human recombinant fluorogenic assay (Trubetskoy *et al.*, 2005; Cohen *et al.*, 2003) ($n = 3$)

[c] Solubility at pH 7.4 in phosphate-buffered saline containing 1 % v/v DMSO

analogs **8a** and **8c**, the mono-methoxy analogs **8b**, **8d**, and **8j** remained highly potent against $hNa_V1.7$ while maintaining reduced CYP3A4 activity. For the pyridyl compounds **8c**, **8e–i,** and **8n**, reduction in CYP3A4 inhibition correlated with reduced $hNa_V1.7$ potency. A combination of electron-withdrawing and electron-donating substituents (**8e–f**, **8l**) retained moderate to good potency on $hNa_V1.7$, suggesting that an H-bond acceptor at either the 3- or 4-positions of the phenyl ring was preferred. Further, substitution with a 3,4-dimethylphenyl group (**8g**) retained potency, but the 3-methyl-4-methoxyphenyl analog (**8h**) was less potent. We also replaced the 5-membered methylenedioxy moiety with an open-chain 2-methoxyethoxy group (**8i**) which retained potency (IC_{50} = 0.15 μM). Also, we noted that, in general, target potency was quite sensitive to the nature of the aryl substituents for a given *N*-substituent. For instance, compound **8d**, bearing an *N*-(pyridyl) methyl substituent along with a single methoxy function on the aryl head was a very potent blocker of $hNa_V1.7$ (IC_{50} = 8 nM); on the other hand, the analogous compounds **8e** (IC_{50} = 0.19 μM) and **8h** (IC_{50} = 1.15 μM) differing from **8d** only by the addition of a fluorine atom and methyl group, respectively, were significantly less potent. The 3,4-difluorophenyl compounds **8a** and **8c** retained some potency against $hNa_V1.7$, whereas the corresponding 3-cyano-4-fluorophenyl compound **8n** was significantly less potent.

These structural modifications were also aimed at attenuating CYP3A4 inhibition potential and enhancing aqueous solubility. Only six compounds (**8c–e**, **8i, 8j**, and **8k**) met the above criteria. Although we were able to obtain highly potent compounds with low CYP3A4 inhibition, such as **8d**, this compound was less efficacious than XEN907 in the complete Freund's adjuvant (CFA) model of inflammatory pain. This lack of in vivo efficacy, in conjunction with the moderate CYP3A4 inhibition and poor solubility, led us to continue our search for a replacement for the methylenedioxy moiety.

The above spirooxindole compounds (**8a–m**) were synthesized in a 5-step process (Scheme 1). Commercially available isatin **2** was converted in high yield to *N*-alkylated isatins **3a–f** using different alkylating agents and NaH in DMF. Following a literature precedent (Hewawasam and Erway, 1998), the substituted phenols **4a–i** were treated with *iso*-PrMgCl at 0 °C for 30 min to generate the corresponding alkoxides which were then combined with *N*-alkyl isatins **3a–f** to provide 3-hydroxy-oxindoles **5a–m** in high yield. Dehydroxylation of compounds **5a–m** was achieved by treatment with triethylsilane and trifluoroacetic acid in dichloromethane to afford compounds **6a–m** in excellent yield (Melch and Williams, 1993; Brueckner *et al.*, 1988). Intermediates **7a–n** were synthesized under Mukaiyama–aldol conditions (silylenol ether generation with TMSCl and an organic base in CH_2Cl_2 at 0 °C for 2 h, followed by

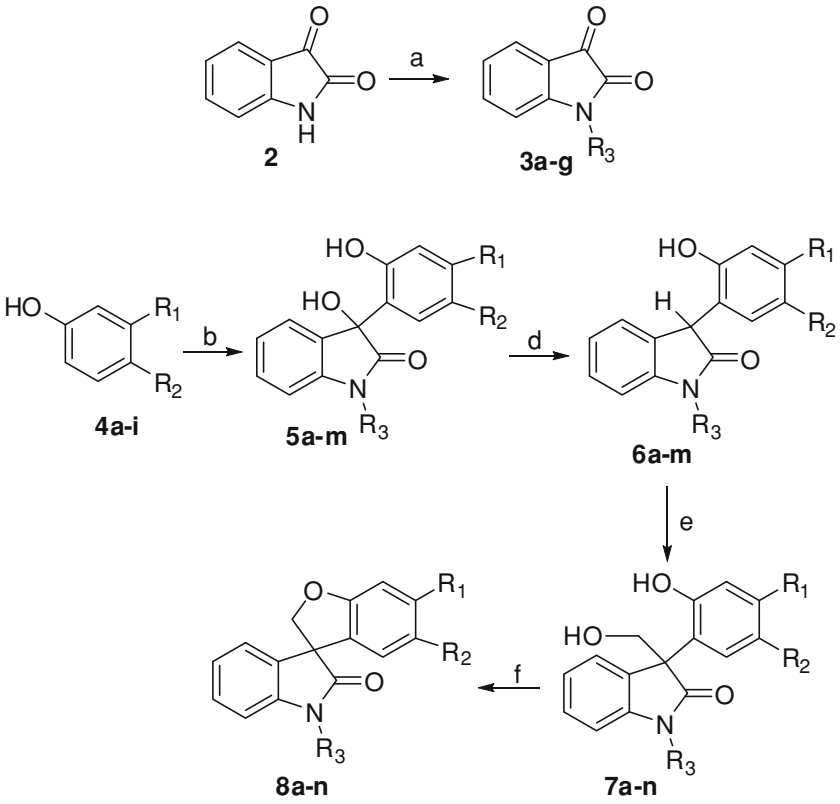

Scheme 1 Reagents and conditions: (*a*) NaH (1.5 eq), DMF, 0 °C, 0.5 h then R^3-X (1.2 eq) (85–98 %); (*b*) *iso*-PrMgCl (1.5 eq), THF, 0 °C, 0.5 h then **3a-f**, 0 °C to rt, 4–16 h (60–85 %); (*d*) TFA, Et_3SiH, CH_2Cl_2, 0 °C to rt, 1–4 h (71–94 %); (*e*) (i) TMSCl, NEt_3, CH_2Cl_2, 0 °C, 2 h; (ii) $(CH_2O)_n$, 37 wt% in H_2O (10 eq), $Yb(OTf)_3$ (cat.), THF, rt, 48 h; (*f*) $(n\text{-}Bu)_3P$, diethyl azodicarboxylate, THF, 0 °C to rt, 16 h (80–90 % over two steps)

reaction with aqueous formaldehyde under $Yb(OTf)_3$ catalysis in THF) (Kobayashi and Hachiya, 1992; Kobayashi *et al.*, 2001). The intramolecular cyclization was achieved by treating hydroxymethylated compounds **7a–n** under Mitsunobu reaction conditions utilizing diethyl azodicarboxylate and $(n\text{-Bu})_3P$ in THF at 0 °C to afford the target spirooxindoles **8a–n** in excellent yield (Swamy *et al.*, 2009).

Further SAR studies were focused on the aryl head group to minimize CYP inhibition and improve solubility. Incorporation of heteroatoms in the aryl head group (Table 2) led to some improvements in both properties. Compounds **17**, **18a–c, 24, 25a,** and **25e–f** have CYP3A4 inhibition values less than 50 % at 10 μM and maintained $hNa_V1.7$ potency. Also, compounds **18d** and **25b–d** are potent blockers of $hNa_V1.7$ and also potent inhibitors of CYP3A4. Interestingly, compound **18d** showed high CYP3A4 inhibition (74 %), whereas **25a** gave only 26 % inhibition with the only difference in structure being the regioisomeric position of the nitrogen in the head group. Although **25a** no longer had a CYP3A4 liability, it was a less potent inhibitor of $hNa_V1.7$ than **18d**. The (*R*)-(tetrahydrofuran-2-yl)methyl *N*-substitution for compounds **8d** (Table 1) and **18a** exhibited very low CYP3A4 inhibition (18 and 14 %, respectively). Similarly, incorporating the (tetrahydro-2*H*-pyran-2-yl)methyl *N*-substituent also reduced the CYP3A4 liabilities for compounds **8e** and **18c** without any loss of potency. These results suggested that a combination of nitrogen substitution at the head group and a polar *N*-substituent was required for low CYP3A4 inhibition.

To our satisfaction, analogs **17**, **18b–c,** and **24** (Table 2) had significantly improved solubility due to the introduction of the additional heteroatom. As shown in Table 2, a non-polar *N*-substituent led to reduced solubility and increased CYP3A4 inhibition. For instance, compounds such as **18d** and **25b–c** had poor solubility and increased CYP3A4 inhibition. The exception was compound **25a** which maintained low CYP3A4 inhibition (26 % at 10 μM).

Of the set of potent blockers of $hNa_V1.7$ in Table 2, **18b** (IC_{50} = 20 nM) had minimal CYP3A4 inhibition and good solubility in phosphate-buffered saline; however, **18b** displayed poor metabolic stability. Compound **18b** was extensively metabolized in rat liver microsomes (RLM) following a 30-min incubation with only 8 % of the parent compound remaining. Furthermore, analog **18b** did not show in vivo efficacy in the CFA-induced inflammatory pain model at doses of 10 and 40 mg/kg (IP and oral, respectively). As previously mentioned, the lack of in vivo efficacy was likely due to poor metabolic stability.

Table 2 Structure-activity relationship of regioisomeric methoxypyridine spirooxindoles (**17**, **18a-d**, **24**, **25a-e**)

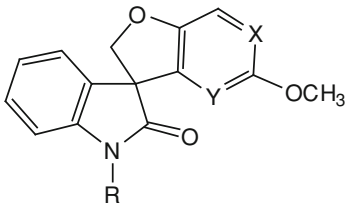

Compound	*X*	*Y*	*R*	$hNa_V1.7$[a] IC_{50} (μM)	CYP3A4, % inhibition at 10 μM[b]	Solubility[c] (μg/mL)
17	N	C	H	0.35	13	52
18a	N	C	(*R*)-Tetrahydrofuran-2-yl)methyl	0.05	14	<5.0
18b	N	C	(*S*)-Tetrahydrofuran-2-yl)methyl	0.02	22	61
18c	N	C	(Tetrahydro-2*H*-pyran-2-yl)methyl	0.10	22	67
18d	N	C	(5-(Trifluoromethyl)furan-2-yl)methyl	0.004	74	<5.0
24	C	N	H	>1.0	27	52
25a	C	N	(5-(Trifluoromethyl)furan-2-yl)methyl	0.13	26	<5.0
25b	C	N	(5-Chlorothiophen-2-yl)methyl	0.06	73	<5.0
25c	C	N	(2-(Isopropyl)thiazole-4-yl)methyl	0.06	70	5
25d	C	N	(2,3-Dihydrobenzo[*b*][1,4]dioxin-6-yl)methyl	0.03	63	5
25e	C	N	(Pyridin-2-yl)methyl	0.18	42	<5.0
25f	C	N	(3-(Trifluoromethyl)pyridin-2-yl)methyl	>0.25	49	<5.0

[a] [^{14}C]guanidinium influx assay adapted for use in HEK-293 cells expressing human $Na_V1.7$ (Reddy *et al.*, 1998)

[b] Human recombinant fluorogenic assay (Trubetskoy *et al.*, 2005; Cohen *et al.*, 2003) (n = 3)

[c] Solubility at pH 7.4 in phosphate-buffered saline containing 1 % v/v DMSO

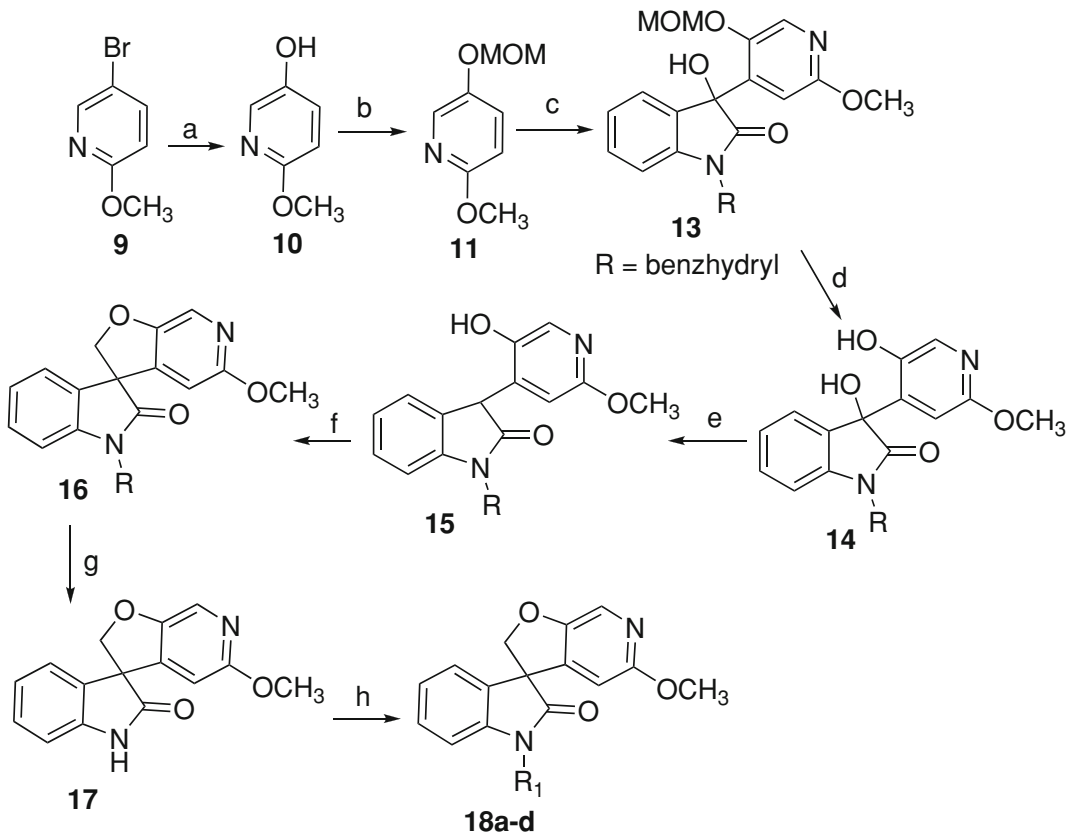

Scheme 2 Reagents and conditions: (*a*) (i) ^{n}BuLi (1.1 eq), THF, −78 °C, 0.5 h, (ii) $B(OCH_3)_3$ (1.25 eq), −78 °C to rt, 9 h, (iii) 35 % aq. H_2O_2 (2.0 eq), 3 h, then acidic workup (91 % over three steps); (*b*) (i) NaH (3.0 eq), 0 °C, THF, 0.5 h, then MOMCl (1.2 eq), 16 h (89 %); (*c*) i. *tert*-BuLi (1.0 eq), THF, −78 °C, 0.5 h, then *N*-benzhydrylisatin (**12**) (1.2 eq), −78 °C to rt, 16 h (64 %); (*d*) TFA/CH_2Cl_2 (1:1), rt, 16 h (98 %); (*e*) (i) $SOCl_2$, NEt_3, DCE, 0 °C to reflux, 1 h, (ii) Zn dust, THF/HOAc (7:1), rt, 16 h (34 % over two steps); (*f*) ICH_2Cl, Cs_2CO_3, THF, rt, 16 h (40 %); (*g*) TFA, Et_3SiH (5 eq), reflux, 8 h (50 %); (*h*) RX or ROTs (1.5–5 eq), Cs_2CO_3 (3 eq), MEK or acetone, reflux, 1.5 h (89–95 %)

Target compounds **17** and **18a–d** (Table 2) were synthesized as shown in Scheme 2. Treatment of the commercially available halide **9** with ^{n}BuLi for 30 min at −78 °C followed by quenching with trimethylborate and oxidation of the borate ester to the corresponding phenol with H_2O_2 afforded intermediate **10** in 91 % yield. The 5-hydroxypyridine **10** was converted to the methoxy methyl ether (MOM) derivative using NaH and MOMCl to afford the protected derivative **11** in 89 % yield. Regioselective *ortho*-lithiation of compound **11** was achieved using *tert*-BuLi at −78 °C for 0.5 h followed by the addition of *N*-benzhydrylisatin **12** to afford intermediate **13** in moderate yield (64 %). The MOM group was removed using TFA in CH_2Cl_2 to obtain intermediate **14** in high yield.

When compound **14** was subjected to similar conditions as depicted in Scheme 1 (i.e., Et_3SiH and TFA in CH_2Cl_2), the expected dehydroxylated product **15** was not formed. To our surprise, we recovered starting material **14** in quantitative yield. Attempts to remove the 3-hydroxyl group of compound **14** turned out to be problematic. Treating **14** with HI did not give any desired product, instead resulting in decomposition of the starting material. Having failed to obtain the desired product **15**, we tried to remove the 3-hydroxyl group by conditions employed by Vedejs in the total synthesis of Diazonamide A (Zajac and Vedejs, 2004). Treating compound **14** with $SOCl_2$ and Et_3N in dichloroethane at reflux afforded the corresponding chloride which was then subjected to Zn dust reduction to afford the desired product **15** in 34 % yield over 2 steps. Compound **15** was treated with chloroiodomethane and Cs_2CO_3 to afford the target compound **16** in 40 % yield. The benzhydryl-protecting group at the *N*-position was removed using Et_3SiH in TFA to provide compound **17** in low yield (38–50 %). Having obtained the key intermediate **17**, we were in a position to explore the substitution at the *N*-position of the spirooxindole. Compounds **18a–d** were obtained in high yield by treating **17** with Cs_2CO_3 and the corresponding alkyl or benzyl halides.

As shown in Scheme 3, compounds **24** and **25a–f** were prepared following a different synthetic pathway than Scheme 2 to improve synthetic feasibility and yields.

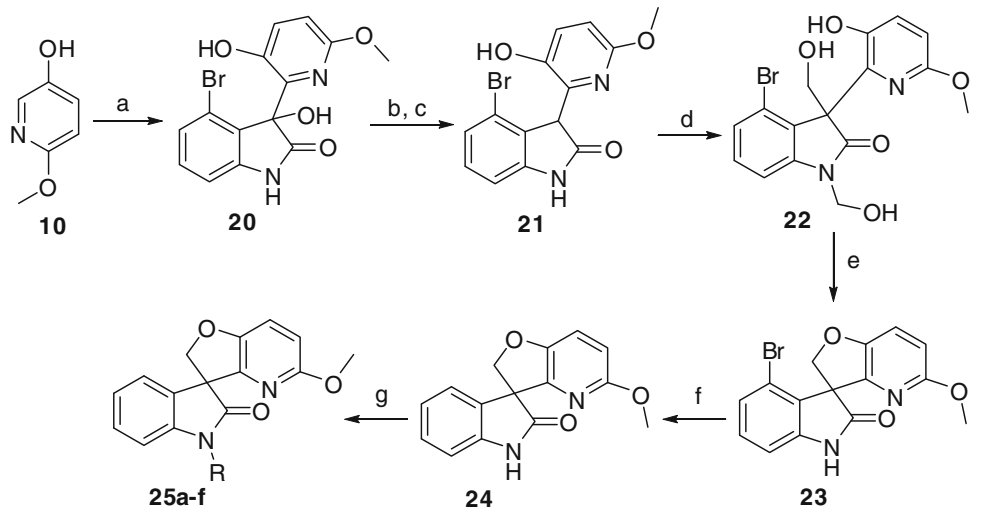

Scheme 3 Reagents and conditions: (*a*) *iso*-PrMgCl (1.5 eq), THF, 0 °C, 0.5 h then 4-bromoisatin (**19**), rt, 4–16 h (60–90 %); (*b*) $SOCl_2$ (2.0 eq), Et_3N (3.0 eq), CH_2Cl_2, 0 °C, 1 h (quant.); (*c*) Zn dust (10 eq), THF–AcOH (9:1), rt, 16 h (80–95 %); (*d*) NaOH (aq.) (4 eq), $(CH_2O)_n$, 37 wt% in H_2O, dioxane, rt, 48 h (quant.); (*e*) $(n\text{-}Bu)_3P$, di-*tert*-butyl azodicarboxylate, THF, 0 °C to rt, 0.5 h (80–90 %); (*f*) $Pd(PPh_3)_4$ (10 mol %), HCO_2H (2 eq), Et_3N (2 eq), dioxane, reflux, 16 h (90–95 %); (*g*) RX (1.2 eq), NaH or Cs_2CO_3 (1.5 eq), DMF, 0 °C to rt, 2–4 h (80–90 %)

Having failed to obtain the product of addition of **10** to isatin **2** in high yield, we investigated the feasibility of this reaction with other substituted isatins. We found that the addition of **10** to 4-substituted isatins gave the best yields. Hence, 5-hydroxypyridine **10** was treated with *iso*-PrMgCl at 0 °C for 0.5 h to generate the alkoxide which was in turn added to 4-bromoisatin **19** to afford intermediate **20** in high yield. The addition of **10** to isatin can take place at both the 4- and 6-positions of the methoxypyridine. The ^1H NMR spectrum of the methoxypyridine adduct contained two doublets assignable to the pyridine ring and was hence diagnostic for structure **20**. In turn, compound **20** was converted to the corresponding chloride using $SOCl_2$ and Et_3N in CH_2Cl_2 and subsequently transformed to compound **21** with 10 equivalents of Zn dust in excellent yield. When compound **21** was treated with aqueous NaOH and *para*-formaldehyde in THF, the diol **22** was obtained in quantitative yield. Compound **22** was subjected to Mitsunobu reaction conditions followed by addition of aqueous NaOH solution to hydrolyze the aminal, affording spirooxindole **23** in 80–90 % yield. Standard palladium-catalyzed dehalogenation using $Pd(PPh_3)_4$, formic acid and Et_3N at reflux in dioxane afforded compound **24** in 95 % yield (Chowdhury *et al.*, 1994). With compound **24** in hand, we introduced different substituents at the *N*-position of the spirooxindole using either NaH or Cs_2CO_3 and an alkylating agent in DMF to obtain compounds **25a–f** in high yield. The regioselectivity of the aforementioned phenol-isatin coupling reaction was confirmed by obtaining a single X-ray crystal structure of compound **25a** (Fig. 2). This crystal structure demonstrated that the addition of the phenol compound **10** to 4-bromoisatin (**19**) occurred at the 6-position (C16 in Fig. 2) rather than at the 4-position (C18). By means of the route depicted in Scheme 3, we were able to prepare large amounts of compound **25a** for further biological evaluation.

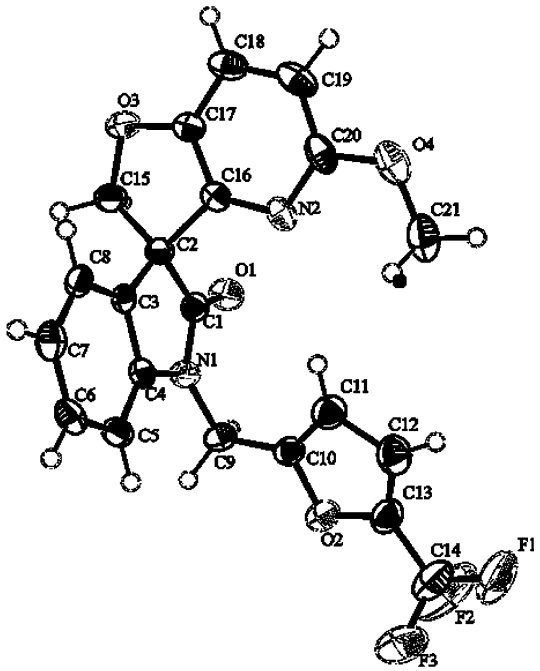

Fig. 2 Single crystal X-ray structure of **25a**

Compound **25a** (Table 3) was not cytotoxic and had favorable hepatocyte metabolic stability in both human and dog. When subjected to rat, human, and dog liver microsome incubations for 60 min (Di *et al.*, 2003), **25a** had 18,

Table 3 ADME properties of **25a**

Property	Value for **25a**
CYP3A4, IC_{50} (μM)[a]	>10
hERG (% Inhibition at 10 μM)[b]	7.5
Solubility (phosphate-buffered saline, pH 7.4) (μg/mL)	<5.0
Plasma protein binding (rat)	95 %
Cytotoxicity (HepG2, % viable after 16 h)	>96 %
Permeability (CaCo-2), P_{app} a → b/b → a (10^{-6} cm/s)	9.1/8.8
Hepatocyte stability, % remaining after 2 h (rat/human/dog)	18/29/49 %

[a] Human recombinant fluorogenic assay (Hewawasam and Erway, 1998) ($n = 3$)

[b] Rb efflux assay (Terstappen, 1998)

29, and 49 %, respectively, of parent compound remaining. Importantly, no meaningful inhibition of CYP3A4 ($IC_{50} > 10$ μM) was observed in a recombinant human enzyme assay. In vivo rat pharmacokinetic data for **25a** are presented in Table 4. When Male Sprague–Dawley rats were dosed *iv* with 1 mg/kg of **25a**, the C_{max} was 884 ng/mL, compared to very low C_{max} (12.7 ng/mL) for oral administration at 10 mg/kg. The clearance for **25a** is high as reflected by a relatively short terminal half-life of about 2 h. Compound **25a** also displayed poor oral bioavailability at 10 mg/kg and the overall pharmacokinetic profile for this compound was not improved over that obtained with our initial spirooxindole $hNa_V1.7$ blocker XEN907 (**1**).

The in vivo efficacy of compound **25a** was evaluated in a CFA-induced inflammatory pain model after oral dosing of male rats at 10 mg/kg. The results are illustrated in Fig. 3. Compound **25a** had a significant analgesic effect at this dose level with a 59 % change from baseline ($p < 0.001$). This level of in vivo efficacy was surprising given its poor pharmacokinetic profile. One possibility was that **25a** might distribute particularly well to peripheral and central nerve tissues. Although further tissue distribution experiments would be required for a definitive confirmation, this possibility was consistent with the steady-state volume of distribution for this compound, which was significantly higher than the rat plasma volume.

Table 4 Mean pharmacokinetic parameters of **25a** after administration to male Sprague–Dawley rats ($n = 2$/group)

Parameter	*po* (10 mg/kg)[a]	*iv* (1 mg/kg)[b]
C_{max} (ng/mL)	12.7	884
AUC_{last} (h•ng/mL)	77.1	244
$t_{½}$ (h)	ND	1.9
T_{max} (h)	4.0	–
V_{ss} (L/kg)	–	4.1
Cl (L/h/kg)	–	4.0
F (%)	3.2	–

[a] Vehicle: labrasol: water: solutol (60:39.5:0.5), dose volume = 5 mL/kg

[b] Vehicle: NMP: solutol: saline (5:20:75), dose volume = 0.5 mL/kg

ND not determined

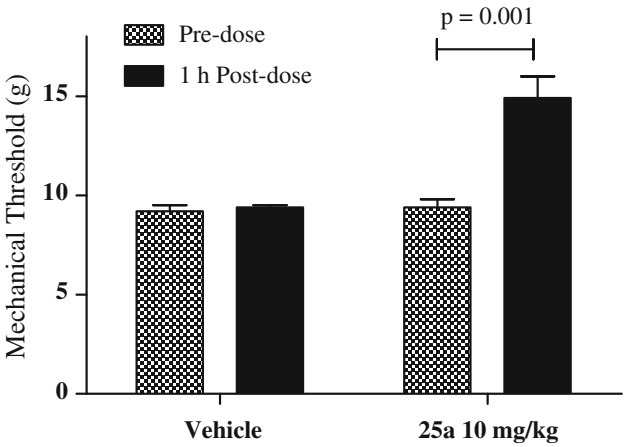

Fig. 3 Mean ± SD von Frey paw withdrawal thresholds in grams for both baseline (i.e., pre-treated) and 1 h post-treatment ($n = 4$/group) with either vehicle or **25a**

Conclusions

In conclusion, we have shown that the tetracyclic spirooxindole compounds **8f** and **18d** are potent $hNa_V1.7$ blockers. During this medicinal chemistry effort, we also identified several compounds, such as **8d**, **8f**, **8k**, **17**, **18a–c**, **24,** and **25a,** that have improved CYP inhibition profiles by virtue of the replacement of the methylenedioxy moiety. Moreover, **25a** was identified as a potent $hNa_V1.7$ blocker with improved ADME profile and significant in vivo efficacy in an inflammatory pain model. Future work in this series of spirooxindoles will focus on further improvements to the pharmacokinetic/pharmacodynamic relationship and will be reported in due course.

Experimental

Chemistry

All reagents were obtained from commercial sources and were either used as supplied or purified by the reported methods. Melting points were determined on a Büchi hot-stage apparatus and are uncorrected. NMR spectra were

recorded on a Bruker Avance 300 spectrometer with chemical shifts (δ) reported in parts-per-million (ppm) relative to the residual signal of the deuterated solvent. Mass spectra were obtained using a Waters 2795/ZQ LC/MS system (Waters Corporation, Milford, MA). HPLC analyses were performed at 25 °C on Agilent 1100 or 1200 systems (Agilent Technologies, Santa Clara, CA) using an EMD Chromolith SpeedROD RP-18e column (4.6 mm i.d. × 50 mm length) (Merck KGaA, Darmstadt, Germany). The mobile phase consisted of a gradient of component "A" (0.1 % v/v aqueous trifluoroacetic acid) and component "B" (acetonitrile) at a flow rate of 1 mL/min. The gradient program used was as follows: initial conditions 5 % B, hold at 5 % B for 1 min., linear ramp from 5 to 95 % B over 5 min, 100 % B for 3 min., and return to initial conditions for 1 min. Peaks were detected at a wavelength of 254 nm using an Agilent photodiode array detector. All compounds reported herein exhibited spectral data consistent with their proposed structures and had HPLC purities in excess of 96 % a/a.

Synthesis of 4-bromo-3-hydroxy-3-(3-hydroxy-6-methoxypyridin-2-yl)-1,3-dihydro-2*H*-indol-2-one (**20**)

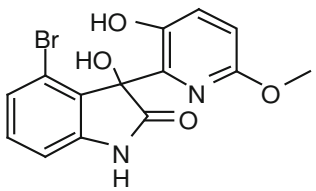

To a pale yellow solution of 5-hydroxy-2-methoxypyridine (**10**) (7.16 g, 57.2 mmol) in anhydrous tetrahydrofuran (100 mL) isopropylmagnesium chloride (28.6 mL, 57.2 mmol, 2.0 M solution in tetrahydrofuran) was added at 0 °C. The resultant solution was stirred for 0.5 h and 4-bromoisatin (10.3 g, 45.8 mmol) was added in portions. The reaction mixture was stirred at ambient temperature for 2 days and 10 % aqueous hydrochloric acid (100 mL) was added. The mixture was extracted with ethyl acetate (3 × 100 mL). The combined organic extracts were dried over anhydrous sodium sulfate, filtered, and concentrated *in vacuo* to dryness. The residue was triturated with diethyl ether to afford the title compound (**20**) (10.7 g, 67 %) as a pale yellow solid: mp 172–175 °C; ^{1}H NMR (300 MHz, DMSO-d_6) δ 10.61 (s, 1H), 9.41 (s, 1H), 7.10 (d, $J = 8.0$ Hz, 2H), 6.99 (d, $J = 8.1$ Hz, 1H), 6.81 (d, $J = 7.6$ Hz, 1H), 6.77 (br s, 1H), 6.68 (d, $J = 8.6$ Hz, 1H), 3.77 (s, 3H); ^{13}C NMR (75 MHz, DMSO-d_6) δ 176.5, 155.5, 145.9, 139.4, 131.6, 128.9, 127.2, 125.6, 118.9, 111.8, 111.1, 109.3, 53.8; MS (ES+) *m*/*z* 352.2 (M + 1), 350.2 (M + 1).

Synthesis of 4-bromo-3-(3-hydroxy-6-methoxypyridin-2-yl)-1,3-dihydro-2*H*-indol-2-one (**21**)

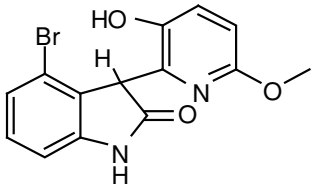

To a solution of 4-bromo-3-hydroxy-3-(3-hydroxy-6-methoxypyridin-2-yl)-1,3-dihydro-2*H*-indol-2-one (**20**) (4.20 g, 12.0 mmol) in anhydrous dichloromethane (100 mL) and anhydrous tetrahydrofuran (10 mL) was added triethylamine (3.64 g, 36.0 mmol) followed by thionyl chloride (4.28 g, 36.0 mmol) at 0 °C. The resultant solution was stirred for 0.5 h at 0 °C and 10 % aqueous hydrochloric acid solution (50 mL) was added. The mixture was extracted with ethyl acetate (3 × 50 mL). The combined organic extracts were washed with saturated ammonium chloride (3 × 50 mL) and brine (50 mL), dried over anhydrous sodium sulfate, and filtered. The filtrate was concentrated *in vacuo* to dryness. The residue was dissolved in tetrahydrofuran (70 mL) and acetic acid (30 mL) and zinc dust (7.84 g, 120 mmol) was added. The reaction mixture was stirred at ambient temperature for 3 h and filtered. The filtrate was concentrated *in vacuo* to dryness. The residue was dissolved in ethyl acetate (100 mL), washed with saturated ammonium chloride (3 × 50 mL) and brine (50 mL), dried over anhydrous sodium sulfate, filtered, and concentrated *in vacuo* to dryness. The residue was purified by column chromatography eluting with ethyl acetate to afford the title compound (**21**) (2.58 g, 64 %) as a pale yellow solid: mp 149–152 °C; ^{1}H NMR (300 MHz, DMSO-d_6) δ 10.61 (s, 1H), 9.34 (br, 1H), 7.15–7.06 (m, 2H), 6.99 (d, $J = 7.8$ Hz, 1H), 6.81 (d, $J = 7.4$ Hz, 1H), 6.55 (d, $J = 8.5$ Hz, 1H), 4.90 (s, 1H), 3.52 (s, 3H); ^{13}C NMR (75 MHz, DMSO-d_6) δ 176.2, 156.5, 147.4, 147.2, 145.7, 138.9, 130.1, 127.7, 124.7, 118.5, 109.7, 108.7, 53.3, 49.4; MS (ES+) *m*/*z* 337.2 (M + 1), 335.2 (M + 1).

Synthesis of 4-bromo-3-(3-hydroxy-6-methoxypyridin-2-yl)-3-(hydroxymethyl)-1,3-dihydro-2*H*-indol-2-one (**22**)

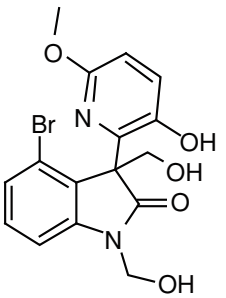

To a mixture of 4-bromo-3-(3-hydroxy-6-methoxypyridin-2-yl)-3-(hydroxymethyl)-1,3-dihydro-2*H*-indol-2-one (**21**) (1.67 g, 5.00 mmol) and *para*-formaldehyde (0.60 g, 20 mmol) in tetrahydrofuran (20 mL) a solution of sodium hydroxide (0.80 g, 20 mmol) in water (10 mL) was added at 0 °C. The reaction mixture was stirred for 1 h at 0 °C and 10 % aqueous hydrochloric acid (50 mL) was added. The mixture was extracted with ethyl acetate (3 × 50 mL). The combined organic extracts were washed with saturated aqueous ammonium chloride (3 × 50 mL) and brine (50 mL), dried over anhydrous sodium sulfate, and filtered. The filtrate was concentrated *in vacuo* to dryness. The residue was purified by column chromatography eluting with 50 % ethyl acetate in hexanes to afford the title compound (**22**) (1.83 g, 81 %) as a colorless solid: mp 142–145 °C; ^{1}H NMR (300 MHz, DMSO-d_6) δ 9.08 (s, 1H), 7.11 (d, $J = 7.8$ Hz, 1H), 7.05 (d, $J = 6.7$ Hz, 1H), 7.00 (dd, $J = 7.8$, 1.0 Hz, 1H), 6.93 (d, $J = 8.7$ Hz, 1H), 6.55 (d, $J = 8.6$ Hz, 1H), 6.23 (br, 1H), 5.09 (d, $J = 10.8$ Hz, 1H), 5.01 (d, $J = 10.6$ Hz, 1H), 4.64 (br, 1H), 4.75 (d, $J = 10.5$ Hz, 1H), 4.29 (d, $J = 10.4$ Hz, 1H), 3.76 (s, 3H); ^{13}C NMR (75 MHz, DMSO-d_6) δ 176.8, 155.5, 147.2, 146.1, 139.5, 129.6, 129.5, 127.2, 125.8, 117.7, 109.7, 108.2, 78.3, 63.5, 63.3, 53.3; MS (ES+) *m*/*z* 419.2 (M + 23), 417.2 (M + 23).

4′-Bromo-5-methoxyspiro[furo[3,2-*b*]pyridine-3,3′-indol]-2′(1′*H*)-one (**23**)

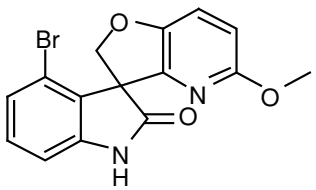

To a solution of 4-bromo-3-(3-hydroxy-6-methoxypyridin-2-yl)-3-(hydroxymethyl)-1,3-dihydro-2*H*-indol-2-one (**22**) (3.48 g, 8.83 mmol) in anhydrous tetrahydrofuran (80 mL) was added tri-*n*-butylphosphine (2.23 g, 11.000 mmol) followed by a solution of di-*tert*-butyl azodicarboxylate (2.54 g, 11.0 mmol) in anhydrous tetrahydrofuran (10 mL) at 0 °C. The mixture was stirred for 1 h at 0 °C, concentrated ammonium hydroxide (5 mL) was added, and stirring was continued for a further 0.5 h at 0 °C. The mixture was concentrated *in vacuo* to dryness. The residue was dissolved in ethyl acetate (100 mL), washed with 10 % aqueous hydrochloric acid (2 × 50 mL), saturated ammonium chloride (30 mL) and brine (30 mL), dried over anhydrous sodium sulfate, and filtered. The filtrate was concentrated *in vacuo* to dryness. The residue was purified by column chromatography eluting with ethyl acetate to afford the title compound (**23**) (1.28 g, 42 %) as a pale yellow solid: mp 265–268 °C; ^{1}H NMR (300 MHz, DMSO-d_6) δ 10.86 (s, 1H), 7.33 (d, $J = 8.8$ Hz, 1H), 7.18 (dd, $J = 7.6$, 7.6 Hz, 1H), 7.10 (d, $J = 8.2$ Hz, 1H), 6.91 (d, $J = 7.5$ Hz, 1H), 6.64 (d, $J = 8.8$ Hz, 1H), 4.80 (d, $J = 9.9$ Hz, 1H), 4.76 (d, $J = 9.9$ Hz, 1H), 3.54 (s, 3H); ^{13}C NMR (75 MHz, DMSO-d_6) δ 177.4, 159.7, 151.1, 144.9, 143.9, 131.2, 130.1, 126.0, 121.4, 119.1, 110.4, 109.8, 76.7, 60.3, 53.9; MS (ES+) *m*/*z* 349.2 (M + 1), 347.2 (M + 1).

Synthesis of 5-methoxyspiro[furo[3,2-*b*]pyridine-3,3′-indol]-2′(1′*H*)-one (**24**)

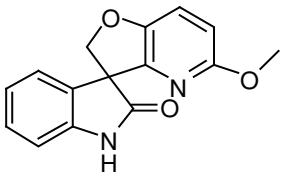

A mixture of 4′-bromo-5-methoxyspiro[furo[3,2-*b*]pyridine-3,3′-indol]-2′(1′*H*)-one (**23**) (1.10 g, 3.18 mmol), *tetrakis*(triphenylphosphine)palladium (0) (0.92 g, 0.79 mmol), formic acid (1.92 g, 41.6 mmol), triethylamine (4.21 g, 41.6 mmol), and anhydrous *p*-dioxane (40 mL) was heated at reflux for 2 h. The hot reaction solution was filtered through a pad of diatomaceous earth. The pad of diatomaceous earth was washed with ethyl acetate (50 mL). The filtrate was concentrated *in vacuo* to dryness. The residue was dissolved in ethyl acetate (50 mL) washed with 10 % aqueous hydrochloric acid (25 mL), saturated ammonium chloride (3 × 15 mL) and brine (3 × 10 mL), dried over anhydrous sodium sulfate, and filtered. The filtrate was concentrated *in vacuo* to dryness. The residue was purified by column chromatography eluting with ethyl acetate to afford the title compound (0.59 g, 69 %) (**24**) as a colorless solid: mp 199–200 °C; ^{1}H NMR (300 MHz, DMSO-d_6) δ 10.62 (s, 1H), 7.38 (d, $J = 8.8$ Hz, 1H), 7.21 (dd, $J = 7.7$, 7.7 Hz, 1H), 7.08 (d, $J = 7.2$ Hz, 1H), 6.94 (d, $J = 7.5$ Hz, 1H), 6.89 (d, $J = 8.0$ Hz, 1H), 6.63 (d, $J = 8.8$ Hz, 1H), 4.83 (d, $J = 9.5$ Hz, 1H), 4.71 (d, $J = 9.5$ Hz, 1H), 3.53 (s, 3H); ^{13}C NMR (75 MHz, DMSO-d_6) δ 177.8, 159.9, 149.8, 146.5, 142.6, 132.1, 129.3, 124.3, 122.7, 121.8, 110.3, 110.2, 79.4, 59.0, 53.9; MS (ES+) *m*/*z* 269.3 (M + 1), 241.3 (M−17).

General procedure A: synthesis of 5-methoxy-1′-{[5-(trifluoromethyl)-2-furyl]methyl}spiro[furo[3,2-*b*]pyridine-3,3′-indol]-2′(1′*H*)-one (**25a**)

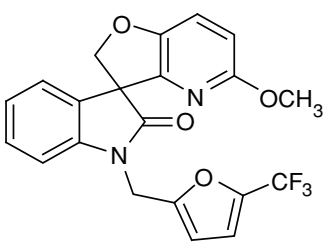

A mixture of 5-methoxyspiro[furo[3,2-*b*]pyridine-3,3′-indol]-2′(1′*H*)-one (**24**) (0.27 g, 1.0 mmol), 4-2-(chloromethyl) -5-(trifluoromethyl)furan (0.18 g, 1.0 mmol) and cesium carbonate (0.32 g, 1.0 mmol) in acetone (2 mL) was stirred at ambient temperature for 16 h. The mixture was filtered and the solid was washed with ethyl acetate (5 mL). The filtrate was concentrated *in vacuo* to dryness. The residue was purified by column chromatography eluting with 30 % ethyl acetate in hexanes to afford the title compound (**25a**) (0.35 g, 83 %) as a colorless solid: mp 145–147 °C; ^{1}H NMR (300 MHz, CD_3CN) δ 7.41 (d, $J = 8.888$ Hz, 1H), (7.30 (dd, $J = 7.7$, 7.7 Hz, 1H), 7.20–7.12 (m, 3H), 7.03 (dd, $J = 7.4$, 7.4 Hz, 1H), 6.67–6.21 m, 2H), 5.15 (d, $J = 16.1$ Hz, 1H), 4.98 (d, $J = 16.2$ Hz, 1H), 4.87 (d, $J = 9.7$ Hz, 1H), 4.78 (d, $J = 9.7$ Hz, 1H), 3.56 (s, 3H); ^{13}C NMR (75 MHz, DMSO-d_6) δ 176.0, 159.9, 153.8, 153.7, 149.7, 146.0, 142.5, 139.8 (m), 131.2, 129.4, 124.3, 123.7, 122.2, 114.5 (m), 110.8, 109.8, 109.7, 79.1, 58.5, 53.6, 37.0; MS (ES+) m/z 417.2 (M + 1).

Synthesis of 1′-[(5-chloro-2-thienyl)methyl]-5-methoxyspiro[furo[3,2-*b*]pyridine-3,3′-indol]-2′(1′*H*)-one (**25b**)

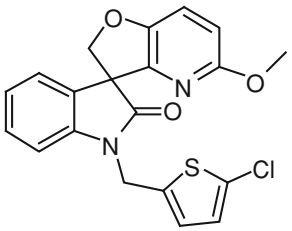

Following general procedure A, compound (**25b**) (0.31 g, 78 %) was obtained as a colorless solid: mp 130–132 °C; ^{1}H NMR (300 MHz, DMSO-d_6) δ 7.41 (d, $J = 8.8$ Hz, 1H), 7.28 (dd, $J = 7.7$, 7.7 Hz, 1H), 7.18 (d, $J = 4.3$ Hz, 1H), 7.16 (d, $J = 4.5$ Hz, 1H), 7.07 (d, $J = 3.8$ Hz, 1H), 7.01 (d, $J = 7.6$ Hz, 1H), 6.94 (d, $J = 3.8$ Hz, 1H), 6.65 (d, $J = 8.8$ Hz, 1H), 5.15 (d, $J = 16.1$ Hz, 1H), 4.98 (d, $J = 16.2$ Hz, 1H), 4.87 (d, $J = 9.7$ Hz, 1H), 4.78 (d, $J = 9.7$ Hz, 1H), 3.52 (s, 3H); ^{13}C NMR (75 MHz, DMSO-d_6) δ 176.0, 159.9, 149.7, 146.1, 142.3, 138.4, 131.3, 129.4, 128.1, 127.1, 126.8, 124.257, 123.7, 122.1, 110.8, 109.9, 79.0, 58.5, 53.7, 38.9; MS (ES+) *m/z* 401.2 (M + 1), 399.2 (M + 1).

Synthesis of 1′-[(2-isopropyl-1,3-thiazol-4-yl)methyl]-5-methoxyspiro[furo[3,2-*b*]pyridine-3,3′-indol]-2′(1′*H*)-one (**25c**)

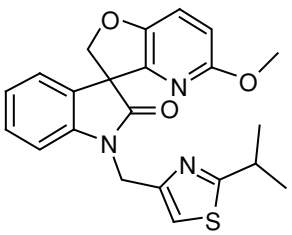

Following general procedure A, the title compound (**25c**) (0.13 g, 64 %) was obtained as a colorless solid: mp 136–138 °C; ^{1}H NMR (300 MHz, DMSO-d_6) δ 7.42 (d, $J = 8.8$ Hz, 1H), 7.29–7.23 (m, 2H), 7.19 (d, $J = 6.8$ Hz, 1H), 7.06–6.99 (m, 2H), 6.65 (d, $J = 8.8$ Hz, 1H), 5.07 (d, $J = 16.4$ Hz, 1H), 4.95 (d, $J = 16.6$ Hz, 1H), 4.89 (d, $J = 9.8$ Hz, 1H), 4.81 (d, $J = 9.7$ Hz, 1H), 3.54 (s, 3H), 3.27–3.18 (m, 1H), 1.28 (d, $J = 6.9$ Hz, 6H); ^{13}C NMR (75 MHz, DMSO-d_6) δ 178.3, 176.1, 159.9, 150.7, 149.7, 146.2, 142.9, 131.3, 129.4, 124.2, 123.6, 122.2, 114.2, 110.8, 109.9, 79.1, 58.6, 53.9, 40.7, 33.0, 23.2; MS (ES+) *m/z* 408.3 (M + 1).

Synthesis of 1′-(2,3-dihydro-1,4-benzodioxin-6-ylmethyl)-5-methoxyspiro[furo[3,2-*b*]pyridine-3,3′-indol]-2′(1′*H*)-one (**25d**)

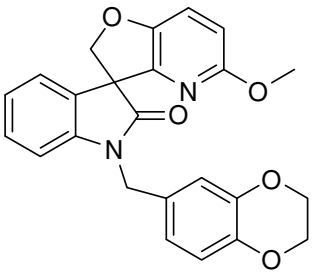

Following general procedure A, the title compound (**25d**) (0.17 g, quantitative yield) was obtained as a colorless solid: mp 144–146 °C (methanol/water); ^{1}H NMR (300 MHz, $CDCl_3$) δ 7.23–7.14 (m, 3H), 7.02 (dd, $J = 7.5$, 7.5 Hz, 1H), 6.94–6.89 (m, 2H), 6.79–6.74 (m, 2H), 6.56 (d, $J = 8.7$ Hz, 1H), 5.26 (d, $J = 15.8$ Hz, 1H), 5.09 (d, $J = 9.3$ Hz, 1H), 4.81 (d, $J = 9.3$ Hz, 1H), 4.57 (d, $J = 15.8$ Hz, 1H), 4.21 (s, 4H), 3.73 (s, 3H); ^{13}C NMR (75 MHz, $CDCl_3$) δ 176.5, 160.4, 149.3, 145.8, 143.9, 143.1, 142.5, 131.8, 129.0, 128.6, 123.6, 123.3, 121.3, 120.1, 117.6, 116.0, 110.7, 109.7, 79.2, 64.4, 59.1, 54.0, 43.5; MS (ES+) *m/z* 416.9 (M + 1).

Synthesis of 5-methoxy-1′-(pyridin-2-ylmethyl)spiro[furo[3,2-*b*]pyridine-3,3′-indol]-2′(1′*H*)-one (**25e**)

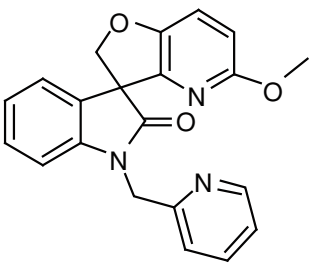

Following general procedure A, the title compound (**25e**) (0.08 g, 75 %) was obtained as a colorless solid: mp 168–171 °C; ^{1}H NMR (300 MHz, DMSO-d_6) δ 8.57 (d, $J = 4.8$ Hz, 1H), 7.72 (dt, $J = 7.7$, 1.8 Hz, 1H), 7.46 (d,

$J = 8.8$ Hz, 1H), 7.37 (d, $J = 7.8$ Hz, 1H), 7.33–7.23 (m, 3H), 7.05 (dt, $J = 7.5$, 0.8 Hz, 1H), 6.94 (d, $J = 7.7$ Hz, 1H), 6.70 (d, $J = 8.8$ Hz, 1H), 5.19 (d, $J = 16.7$ Hz, 1H), 4.97–4.86 (m, 3H), 3.62 (s, 3H); ^{13}C NMR (75 MHz, DMSO-d_6) δ 175.8, 159.4, 155.4, 149.4, 149.1, 145.7, 142.5, 137.0, 130.8, 128.9, 123.7, 123.0, 122.6, 121.7, 120.3, 110.2, 109.3, 78.5, 58.1, 53.3, 44.9; MS (ES+) *m/z* 360.4 (M + 1).

Synthesis of 5-methoxy-1′-((3-(trifluoromethyl)pyridin-2-yl)methyl)-2*H*-spiro[furo[3,2-b]pyridine-3,3′-indolin]-2′-one (**25f**)

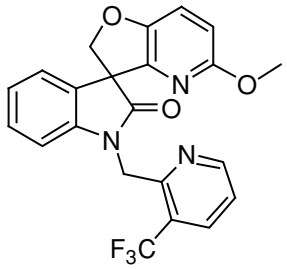

Following general procedure A, the title compound (**25f**) (0.15 g, 76 %) was obtained as a colorless solid: mp 195–198 °C; ^{1}H NMR (300 MHz, DMSO-d_6) δ 8.68 (d, $J = 4.4$ Hz, 1H), 8.23 (d, $J = 7.2$ Hz, 1H), 7.54 (dd, $J = 7.8$, 4.9 Hz, 1H), 7.45 (d, $J = 8.8$ Hz, 1H), 7.30 (ddd, $J = 8.2$, 8.2, 5.8 Hz, 1H), 7.23 (d, $J = 6.6$ Hz, 1H), 7.04 (dd, $J = 7.5$ Hz, 1H), 6.94 (d, $J = 7.8$ Hz, 1H), 6.69 (d, $J = 8.8$ Hz, 1H), 5.25 (s, 2H), 4.86 (d, $J = 9.5$ Hz, 2H), 3.61 (s, 3H); ^{13}C NMR (75 MHz, DMSO-d_6) δ 176.2, 159.3, 152.6, 152.4, 152.3, 149.5, 145.3, 143.5, 134.7 (q, $^4J_{C-F} = 4.9$ Hz), 130.3, 128.9, 128.8, 125.6 (q, $^1J_{C-F} = 274$ Hz), 123.7, 122.8, 121.4, 109.9, 109.2, 79.2, 58.0, 53.3, 42.2; MS (ES+) *m/z* 427.2 (M + 1), 449.2 (M + 23).

Pharmacology

Guanidinium influx assay

All IC_{50} data reported herein are means of no fewer than two replicate experiments. Briefly, cells expressing $hNa_V1.7$ were plated on a PDL-coated Scintiplate (PerkinElmer, Waltham, MA) at a density of $\sim 10^6$ cells/well and incubated overnight (37 °C, 5 % CO_2). Cells were washed with low-sodium HEPES-buffered saline solution (LHNBSS) assay buffer (150 mM choline chloride, 20 mM HEPES, 1 mM $CaCl_2$, 5 mM KCl, 1 mM $MgCl_2$, 10 mM glucose, adjusted with Tris to pH 7.4). Test compounds were added in DMSO (final assay DMSO concentration 0.5 %), followed by [^{14}C] guanidinium chloride (0.05 μCi/well, American Radiolabeled Chemicals, St. Louis, MO) and aconitine (final concentration 10 μM, Cedarlane Laboratories, Burlington, ON). The plate was incubated for 2 h at ambient temperature, after which time the plates were washed with LHNBSS + 10 mM guanidinium chloride. Residual volumes were removed and air dried overnight. Plates were read the following day on a Wallac MicroBeta TriLux liquid scintillation counter (PerkinElmer, Waltham, MA).

CFA assay

Complete Freund's adjuvant (CFA) (Sigma-Aldrich Canada, Oakville, ON) was suspended in a mineral oil/saline (1:1 v/v) emulsion at a concentration of 0.5 mg/mL. Under light isoflurane anesthesia, 150 μL of the CFA emulsion was injected subcutaneously into the plantar surface of the rat's left hind paw. At 7 days post-injection, animals were screened for CFA-induced inflammatory mechanical allodynia by the von Frey test as described below. Only animals with significant allodynia were enrolled in the study. The paw withdrawal threshold of animals to mechanical tactile stimuli was measured using the Model 2290 Electrovonfrey anesthesiometer (IITC Life Science, Woodland Hills, CA). Animals were placed in an elevated acrylic enclosure set on a wire mesh surface. After 20 min of acclimation, a #13 Von Frey tip was applied perpendicularly to the plantar surface of the ipsilateral hind paw of the animals with sufficient force to elicit a crisp flickering response of the paw, indicating a withdrawal response from pain that defined the experimental endpoint. A total of five readings were taken from each animal with an interval of 1 min between the readings. The force (in grams) required to elicit the withdrawal response was recorded both before (baseline measurement) and 1 h after test article dosing.

Human recombinant CYP fluorogenic assay

This assay is based on the cytochrome P450 inhibition kit described by Vivid CYP450 Screening kit protocol, 2005, Invitrogen Corporation (Invitrogen Corporation, 1600 Faraday Avenue, Carlsbad, California, 92008, USA).

Rb efflux assay

HEK293 cells stably expressing the hERG potassium channel were plated on a PDL-coated 96-well plate (Becton–Dickinson, 1 Becton Drive, Franklin Lakes, New Jersey, 07417, USA) at a density of 10^6 cells/well and incubated overnight (37 °C, 5 % CO_2). Cells were loaded with Rb loading buffer (5.4 mM RbCl, 150 mM NaCl, 2 mM $CaCl_2$, 0.8 mM NaH_2PO_4, 1 mM $MgCl_2$, 5 mM glucose, 25 mM HEPES adjusted with Tris to pH 7.4) and incubated for 3 h (37 °C, 5 % CO_2). Test compounds were added in DMSO (final assay DMSO concentration 0.5 %) during the last 30 min of loading. The Rb loading buffer was then removed and cells were washed twice with 200 uL of wash buffer (5.4 mM KCl,

150 mM NaCl, 2 mM $CaCl_2$, 0.8 mM NaH_2PO_4, 1 mM $MgCl_2$, 5 mM glucose, 25 mM HEPES adjusted with Tris to pH 7.4). The hERG channel was activated with 200 uL 0.1 M KCl for 4 min. The supernatant was collected and cells were lysed with 1 % Triton X 100. The Rb^+ concentration in the supernatant and cell lysates was measured by atomic absorption. The amount of Rb^+ efflux was calculated for each sample relative to control (DMSO).

Acknowledgments The authors are grateful to Drs. Michael Winther and Rostam Namdari of ADME group for their support. The authors are also thanks to Drs. Tarek Mansour and Renata Oballa for their help and critical discussion to write the manuscript.

References

Brueckner C, Holzinger H, Reissig HU (1988) Diastereoselective syntheses of highly substituted methyl tetrahydrofuran-3-carboxylates by reaction of gamma-lactols with silylated nucleophiles. J Org Chem 52:2450–2456. doi:10.1021/jo00246a011

Castro A et al (2003) Synthesis and cytotoxicity of podophyllotoxin analogues modified in the A ring. Eur J Med Chem 38:65–74. doi:10.1016/S0223-5234(02)00007-7

Cohen LH, Remley MJ, Raunig D, Vaz AD (2003) In vitro drug interactions of cytochrome p450: an evaluation of fluorogenic to conventional substrates. Drug Metab Dispos 10:1005–1015. doi:10.1124/dmd.31.8.1005

Chowdhury S et al (2011) Discovery of XEN907, a spirooxindole blocker of NaV1.7 for the treatment of pain. Bioorg Med Chem Lett 21:3676–3681. doi:10.1016/j.bmcl.2011.04.088

Chowdhury S, Zhao BP, Snieckus V (1994) Abbreviated synthesis of benzo[c]phenanthrene, benz[a]anthracene and their respective 5-methyl derivatives via combined metalation-palladium-catalyzed cross coupling strategy. Polycyclic Aromat Compd 5:27–34. doi:10.1080/10406639408015152

Cox JJ, Reimann F, Nicholas AK et al (2006) An SCN9A channelopathy causes congenital inability to experience pain. Nature 444:894–898. doi:10.1038/nature05413

Cummins TR, Dib-Hajj SD, Waxman SG (2004) Electrophysiological properties of mutant Nav1.7 sodium channels in a painful inherited neuropathy. J Neurosci 24:8232–8236. doi:10.1523/jneurosci.2695-04.2004

Cummins TR, Sheets PE, Waxman SG (2007) The roles of sodium channels in nociception: implications for mechanisms of pain. Pain 131:243–257. doi:10.1016/j.pain.2007.07.026

Di L, Kerns EH, Hong Y, Kleintop TA, McConnell OJ, Huryn DM (2003) Optimization of a higher throughput microsomal stability screening assay for profiling drug discovery candidates. J Biomol Screen 8:453–462. doi:10.1177/1087057103255988

Fertleman CR, Baker MD, Parker KA, Moffat S et al (2006) SCN9A mutations in paroxysmal extreme pain disorder: allelic variants underlie distinct channel defects and phenotypes. Neuron 52:767–774. doi:10.1016/j.neuron.2006.10.006

Reimann F, Cox JJ, Belfer I et al (2010) Pain perception is altered by a nucleotide polymorphism in SCN9A. PNAS 107:5148–5153. doi:10.1073/pnas.0913181107

Ghelardini C, Desphy JF, Muraglia M, Corbo C, Matucci R, Dipalma a, Bertucci C, Pistolozzi M, Nesi M, Norcini M, Franchini C, Camerino DC (2010) Effects of a new potent analog of tocainide on hNav1.7 sodium channels and in vivo neuropathic pain models. Neuroscience 169:863–873. doi:10.1016/j.neuroscience.2010.05.019

Goldberg YP et al (2007) Loss-of-function mutations in the Nav1.7 gene underlie congenital indifference to pain in multiple human populations. Clin Genet 71:311–319. doi:10.1111/j.1399-0004.2007.00790.x

Hewawasam P, Erway M (1998) Reactivity and regioselectivity of magnesium phenolates towards isatins: one-step synthesis of 3-(2-hydroxyaryl)-3-hydroxyindolones. Tetrahedron Lett 39:3981–3984. doi:org/10.1016/S0040-4039(98)00741-2

Imperio D et al (2007) Replacement of the lactone moiety on podophyllotoxin and steganacin analogues with a 1,5-disubstituted 1,2,3-triazole via ruthenium-catalyzed click chemistry. Bioorg Med Chem 15:6748–6757. doi:org/10.1016/j.bmc.2007.08.020

Klugbauer N, Lacinova L, Flockerzi V, Hofmann F (1995) Structure and functional expression of a new member of the tetrodotoxin-sensitive voltage-activated sodium channel family from human neuroendocrine cells. EMBO J 14:1084–1090

Kobayashi S, Hachiya I (1992) The aldol reaction of silyl enol ethers with aldehydes in aqueous media. Tetrahedron Lett 33:1625–1633. doi:org/10.1016/S0040-4039(00)91691-5

Kobayashi S, Hamada T, Nagayama S, Manabe K (2001) Lanthanide trifluoromethanesulfonate-catalyzed asymmetric aldol reactions in aqueous media. Org Lett 3:165–167. doi:10.1021/ol006830z

Melch WM, Williams MT (1993) Synthesis of 7-3H-(IS, 4S)-4-(3,4-dichlorophenyl)-1,2,3,4-tetrahydro-*N*-methyl-I-I-naphthalenamine hydrochloride (7-3H-Sertraline. J Labelled Compd Radiopharm 33:119–125. doi:10.1002/jlcr.2580330206

Reddy NL et al (1998) Synthesis and pharmacological evaluation of *N*, *N*′-diarylguanidines as potent sodium channel blockers and anticonvulsant agents. J Med Chem 41:3298–3302. doi:10.1021/jm980134b

Sangameswaran L, Fish LM, Koch BD et al (1997) A novel tetrodotoxin-sensitive, voltage-gated sodium channel expressed in rat and human dorsal root ganglia. J Biol Chem 272:14805–14809. doi:10.1074/jbc.272.23.14805

Toledo-Aral JJ, Moss BL, He ZJ, Koszowski AG, Whisenand T, Levinson SR, Wolf JJ, Silos-Santiago I, Halegoua S, Mandel G (1997) Identification of PN1, a predominant voltage-dependent sodium channel expressed principally in peripheral neurons. Proc Natl Acad Sci USA 94:1527–1532

Staack RF, Maurer HH (2005) Metabolism of designer drugs of abuse. Curr Drug Metab 6:259–274

Swamy KCK, Kumar NNB, Balaraman E, Kumar KVPP (2009) Mitsunobu and related reactions: advances and applications. Chem Rev 109:25512651. doi:10.1021/cr800278z

Terstappen GC (1998) Functional analysis of native and recombinant ion channels using a high-capacity nonradioactive rubidium efflux assay. Anal Biochem 272:149–155. doi:org/10.1006/abio.1999.4179

Trubetskoy et al (2005) Highly miniaturized formats for in vitro drug metabolism assays using vivid fluorescent substrates and recombinant human cytochrome P450 enzymes. J Biomol Screen 10:56–66. doi:10.1177/1087057104269731

Yang Y et al (2004) Mutations in SCN9A, encoding a sodium channel alpha subunit, in patients with primary erythermalgia. J Med Genet 41:171–174. doi:10.1136/jmg.2003.012153

Zajac MA, Vedejs E (2004) A synthesis of the diazonamide heteroaromatic biaryl macrocycle/hemiaminal core. Org Lett 6:237–240. doi:10.1021/ol036179a

Zhang L, Wang WH, Li LF, Dong GX, Zhao J, Luan JY, Sun TT (2010) Long-term remission of primary erythermalgia with R1150W polymorphism in SCN9A after chemical lumbar sympathectomy. Eur J Dermatol 20:763–767. doi:10.1177/1358863X11422584

Zuliani V, Rivara M, Fantini M, Costantino G (2010) Sodium channel blockers for neuropathatic pain. Expert Opin Ther Patents 20:755–779. doi:10.1517/13543771003774118